Received: 8 July 2022 | Revised: 6 November 2022 | Accepted: 7 November 2022

DOI: 10.1002/ntls.20220035

RESEARCH ARTICLE

Natural Sciences

Hot exciton effect in photoluminescence of monolayer transition metal dichalcogenide

Ke Xiao[1] | **Ruihuan Duan**[2] | **Zheng Liu**[2] | **Kenji Watanabe**[3] | **Takashi Taniguchi**[4] | **Wang Yao**[1] | **Xiaodong Cui**[1]

[1]Department of Physics, The University of Hong Kong, Hong Kong, China

[2]School of Materials Science and Engineering, Nanyang Technological University, Singapore, Singapore

[3]Research Center for Functional Materials, National Institute for Materials Science, Tsukuba, Japan

[4]International Center for Materials Nanoarchitectonics, National Institute for Materials Science, Tsukuba, Japan

Correspondence
Xiaodong Cui, Department of Physics, The University of Hong Kong, Hong Kong, China.
Email: xdcui@hku.hk

Funding information
Hong Kong University Grants Council/ Research grants council under schemes of, Grant/Award Number: AoE/P-701/20; GRF, Grant/Award Number: 17300520; AoE seed fund of the University of Hong Kong and National Key R&D Program of China, Grant/Award Number: 2020YFA0309600; Elemental Strategy Initiative conducted by the MEXT, Japan, Grant/Award Number: JPMXP0112101001; JSPS KAKENHI, Grant/Award Numbers: 19H05790, 20H00354, 21H05233; Singapore Ministry of Education Tier 3 Programme "Geometrical Quantum Materials" AcRF Tier 3, Grant/Award Number: MOE2018-T3-1-002; AcRF Tier 2, Grant/Award Number: MOE2019-T2-2-105

Abstract

Hot excitons are usually neglected in optical spectroscopy in two-dimensional semiconductors for the sake of momentum conservation, as the majority of hot excitons are out of light cones. In this letter, we elaborate on the contribution of hot excitons to optical properties of monolayer Molybdenum diselenide ($MoSe_2$) with photoluminescence (PL) and PL excitation (PLE) spectroscopy. With the excitation-intensity-dependent PL, temperature-dependent PL and PLE experiments combined with the simulations, we experimentally distinguish the influences of the exciton temperature and the lattice temperature in the PL spectrum. It is concluded that the acoustic phonon-assisted PL accounts for the non-Lorentzian high energy tail in the PL spectrum, and the hot exciton effect is significant to linear optical properties of transition metal dichalcogenides. Besides, the effective exciton temperature is found to be several tens of Kelvin higher than the lattice temperature at non-resonant optical excitation. It indicates that the exciton temperature needs to be carefully taken into account when considering the exciton-related quantum phase phenomena such as exciton condensation. It is experimentally demonstrated that the effective exciton temperature can be tuned by excitation energy.

Key points:

- The acoustic phonon-assisted photoluminescence (PL) accounts for the non-Lorentzian high-energy tail in the PL spectrum.
- "Hot" excitons play a significant role in optical properties of two-dimensional transition metal dichalcogenides.
- The effective exciton temperature could be tuned by excitation energy.

KEYWORDS
2D semiconductors, exciton-phonon coupling, hot exciton

This is an open access article under the terms of the Creative Commons Attribution License, which permits use, distribution and reproduction in any medium, provided the original work is properly cited.
© 2022 The Authors. *Natural Sciences* published by Wiley-VCH GmbH.

26986248, 2023, 1, Downloaded from https://onlinelibrary.wiley.com/doi/10.1002/ntls.20220035 by Cochrane Japan, Wiley Online Library on [13/01/2023]. See the Terms and Conditions (https://onlinelibrary.wiley.com/terms-and-conditions) on Wiley Online Library for rules of use; OA articles are governed by the applicable Creative Commons License

INTRODUCTION

Monolayer transition metal dichalcogenides (TMDs) have been recognized as one of the superior playgrounds for two-dimensional (2D) physics, particularly 2D exciton study. The weak Coulomb screening and 2D nature lead to prominent excitons with a giant binding energy dominating monolayer TMDs' optical properties.[1–6] The attributes of excitons in monolayer TMDs featuring strong oscillator strength, richness of degrees of freedom, that is, spin and valley, and spin-valley locking[7,8] have been stimulating intriguing experiments in many-body physics.[9,10] Especially, the strong spin–orbit coupling of the transition metal atoms gives rise to the large spin splitting in the valence band, resulting in the two families of optical accessible bright excitons, namely, A excitons (lower energy) and B excitons (higher energy).[11,12] As yet, not much attention has been paid to the influence of hot excitons whose kinetic energy is significantly higher than lattice temperature. Unlike hot electrons that affect physics properties in many aspects,[13–15] hot excitons are usually neglected in optical spectroscopy except in dynamics study[16] for the sake of momentum conservation, as the majority of hot excitons are out of light cone. Figure 1 depicts the photoluminescence (PL) process in TMDs. The excited electrons and holes immediately form excitons in a highly non-equilibrium state once pumped as Figure 1a elaborates. After a time τ_{th}(~sub-100*fs*),[17,18] a thermalization among excitons themselves is reached, and excitons follow the Boson/Boltzmann distribution characterized by the exciton temperature $T_{exciton}$ (Figure 1b). Note that the exciton temperature is still much higher than the lattice temperature $T_{lattice}$ at this time. The excitons further cool down accompanying with an energy transfer to lattice via exciton-phonon scattering or some other process[19–21] until achieving thermal equilibrium ($T_{exciton} = T_{lattice}$), characterized by a time scale τ_{ex-ph} (~tens of picosecond; Figure 1c).[16,22–25]

It is widely assumed that excitons and lattices share the same temperature in optical spectroscopy. Given that the excitons' radiative lifetime of sub-picosecond[26] is much shorter than τ_{ex-ph}, the excitons could radiate before thermalizing with the lattice. Meanwhile, only the excitons inside the light cone can realize direct radiative recombination for the requirement of in-plane momentum conservation (Figure 1d). Intuitively, the temperature of excitons seems not as important as that of electrons since these radiation-active excitons are much less influenced by the exciton temperature. The homogeneous linewidth broadening (~several meV) can also relax to some extent the energy-momentum conservation requirement in the exciton's light emission.[27] We calculate the PL spectra at various exciton temperatures ($T_{exciton}$) and conclude this homogeneous linewidth broadening effect is considerably minor and has a negligible contribution to the PL linewidth (more specifically in the Supporting Information). The other mechanism accounting for the linewidth broadening is the acoustic phonon-assisted exciton PL.[28–30] The hot excitons (green circle in Figure 1d) could be scattered into the light cone by absorbing or emitting acoustic phonons.

In this letter, we elaborate the contribution of hot excitons to optical properties of monolayer $MoSe_2$. With the intensity- and temperature-dependent PL and PL excitation (PLE) experiments combined with the simulations, we experimentally distinguish the influences of the exciton temperature and the lattice temperature in the PL spectrum. It is concluded that the acoustic phonon assisted PL (APAPL) accounts for the non-Lorentzian high-energy tail in the PL spectrum, and the hot exciton effect is significant to optical properties of TMDs. Besides, the

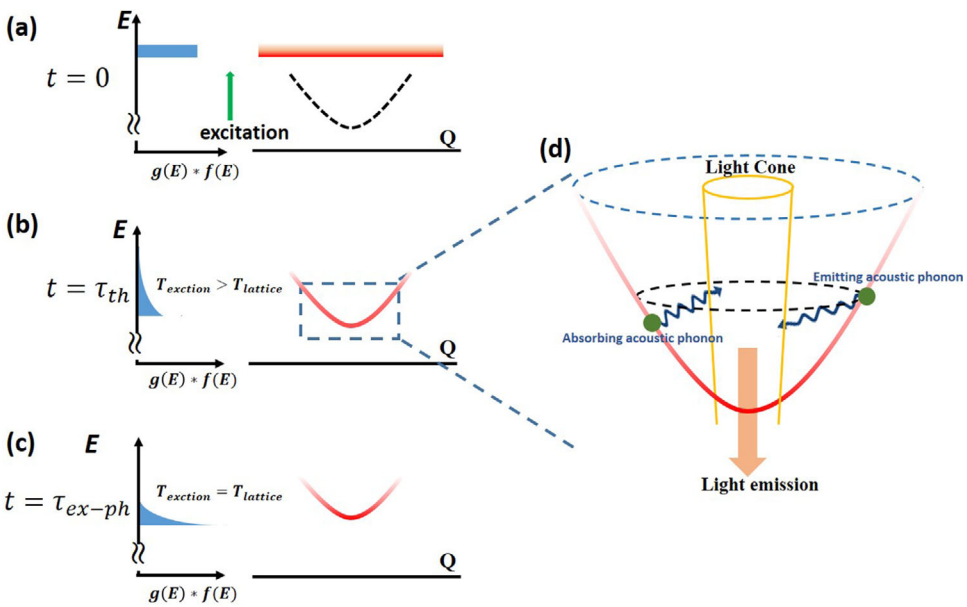

FIGURE 1 Schematic of the exciton distribution dynamics. (a) at $t = 0$, excitons are in a highly non-equilibrium state after a pulse excitation. (b) at $t = \tau_{th}$, the excitons reach thermalization of themselves at $T_{exciton} > T_{lattice}$. (c) at $= \tau_{ex-ph}$, the exciton temperature cools down and achieves a thermal equilibrium with lattice. $g(E)$ and $f(E)$ represent the density of states and Boltzmann distribution respectively. Q is the center of mass momentum of excitons. The line-thickness of the exciton dispersion (in red) represents the effective occupation. (d) Zoom-in of the dashed area in (b) sketches acoustic phonon-assisted exciton photoluminescence (PL)

26986248, 2023, 1, Downloaded from https://onlinelibrary.wiley.com/doi/10.1002/ntls.20220035 by Cochrane Japan, Wiley Online Library on [13/01/2023]. See the Terms and Conditions (https://onlinelibrary.wiley.com/terms-and-conditions) on Wiley Online Library for rules of use; OA articles are governed by the applicable Creative Commons License

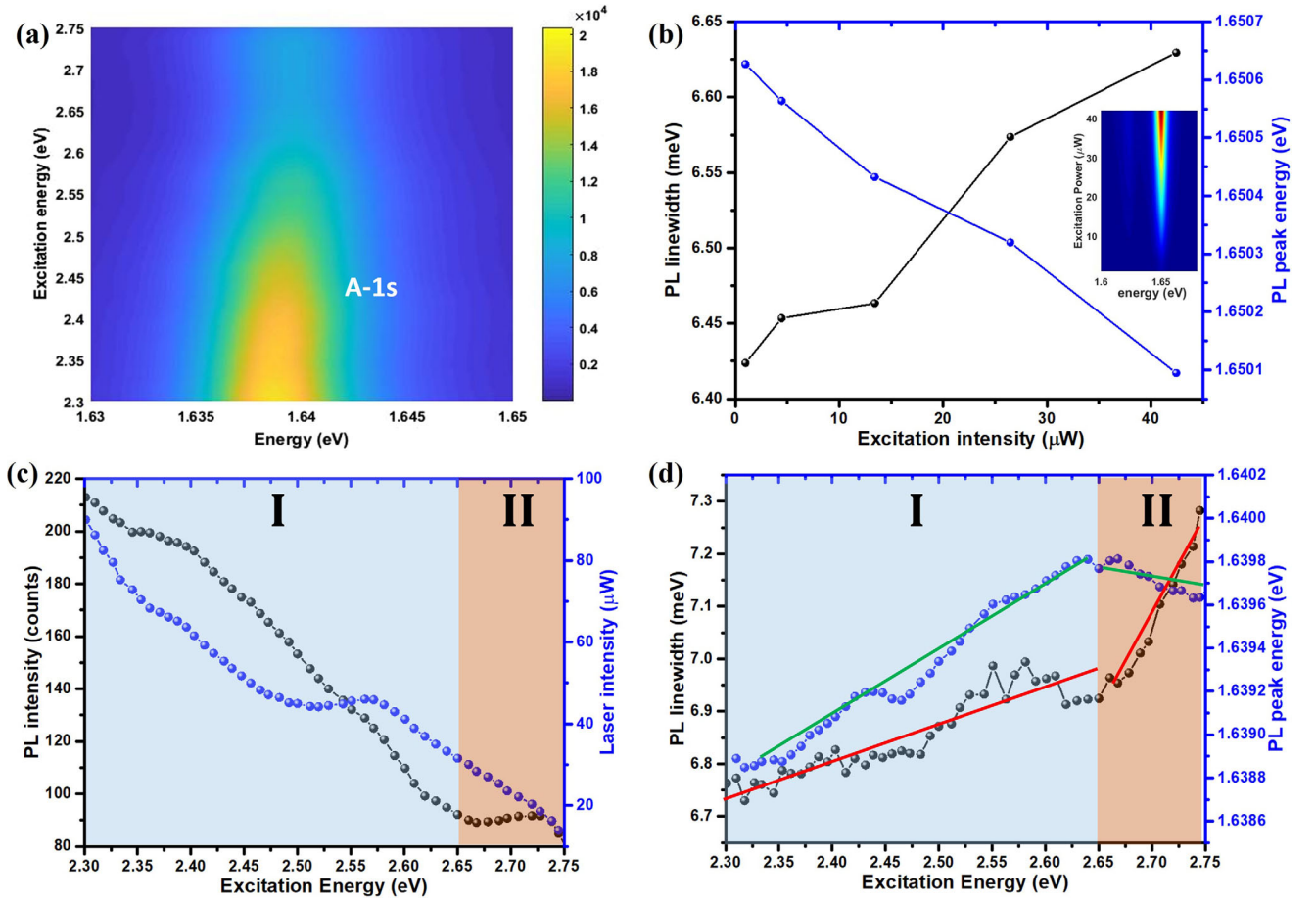

FIGURE 2 (a) PL excitation (PLE) spectral map of $MoSe_2$ with the excitation energy ranging from 2.3 to 2.75 eV. Lorentz fitting results: PL intensity (c), PL peak energy and PL linewidth (d) are summarized as a function of excitation energy. (c) and (d) are further divided into two regions based on the PL intensity. (b) The PL linewidth and PL energy peak (determined by Lorentz fitting) as a function of excitation intensity. The inset shows the two-dimensional map of excitation-intensity-dependent PL spectra. The excitation-intensity-dependent PL is measured under an excitation of 2.33 eV at 15 K

contrasting linewidth broadening behaviors owing to exciton temperature increase or lattice temperature increase are discussed. It is experimentally demonstrated that the effective exciton temperature can be tuned by excitation energy.

RESULTS

Figure 2 summarizes our PLE and excitation-intensity-dependent PL data. The excitation energy ranging from 2.3 to 2.75 eV is set far beyond the A and B exciton energies to avoid resonant absorption. The excitation intensity is kept below 100 —W to minimize the local heating. The PL intensity across the excitation range primarily results from the corresponding excitation intensity profile (blue ball in Figure 2c) and the absorption coefficient (details in the Supporting Information). At region I, the PL intensity decreases as the excitation energy increases primarily owing to the reduction of laser intensity (blue balls in Figure 2c). At region II, the PL intensity remains unchanged relatively and even slightly increases though the excitation intensity reduces with the increase energy, which may result from the boosted absorption in C band (more details in the Supporting Information). The energy shift of *A-1s* exciton shows a consistent trend with PL intensity or exciton density, which also agrees well with our excitation-intensity-dependent PL result (Figure 2b). In Figure 2b, the *A-1s* peak energy undergoes a slight redshift with the increase of exciton density under the excitation of 2.33 eV accompanying the linewidth broadening, which is consistent with the previous results.[31] The redshift is attributed to the bandgap renormalization and Coulomb screening effect. Usually, as the excitation intensity increases, the electronic bandgap decreases owing to the bandgap renormalization from photocarriers,[32–35] whereas the Coulomb screening effect is enhanced owing to the increased exciton density, leading to the decrease of the exciton binding energy, and consequently results in the PL peak energy blueshift.[35] In monolayer $MoSe_2$, the bandgap renormalization effect is larger than the Coulomb screening effect, and therefore the PL peak undergoes a redshift as a function of excitation intensity. Figure 2d indicates that the excitation energy plays a more prominent role at low exciton density. Usually, a low-intensity excitation leads to narrower exciton PL linewidth on account of the less Auger-like exciton–exciton interaction[26,36] as elaborated in Figure 2b. In region I, although the PL intensity or exciton

26986248, 2023, 1, Downloaded from https://onlinelibrary.wiley.com/doi/10.1002/nts.20220035 by Cochrane Japan, Wiley Online Library on [13/01/2023]. See the Terms and Conditions (https://onlinelibrary.wiley.com/terms-and-conditions) on Wiley Online Library for rules of use; OA articles are governed by the applicable Creative Commons License

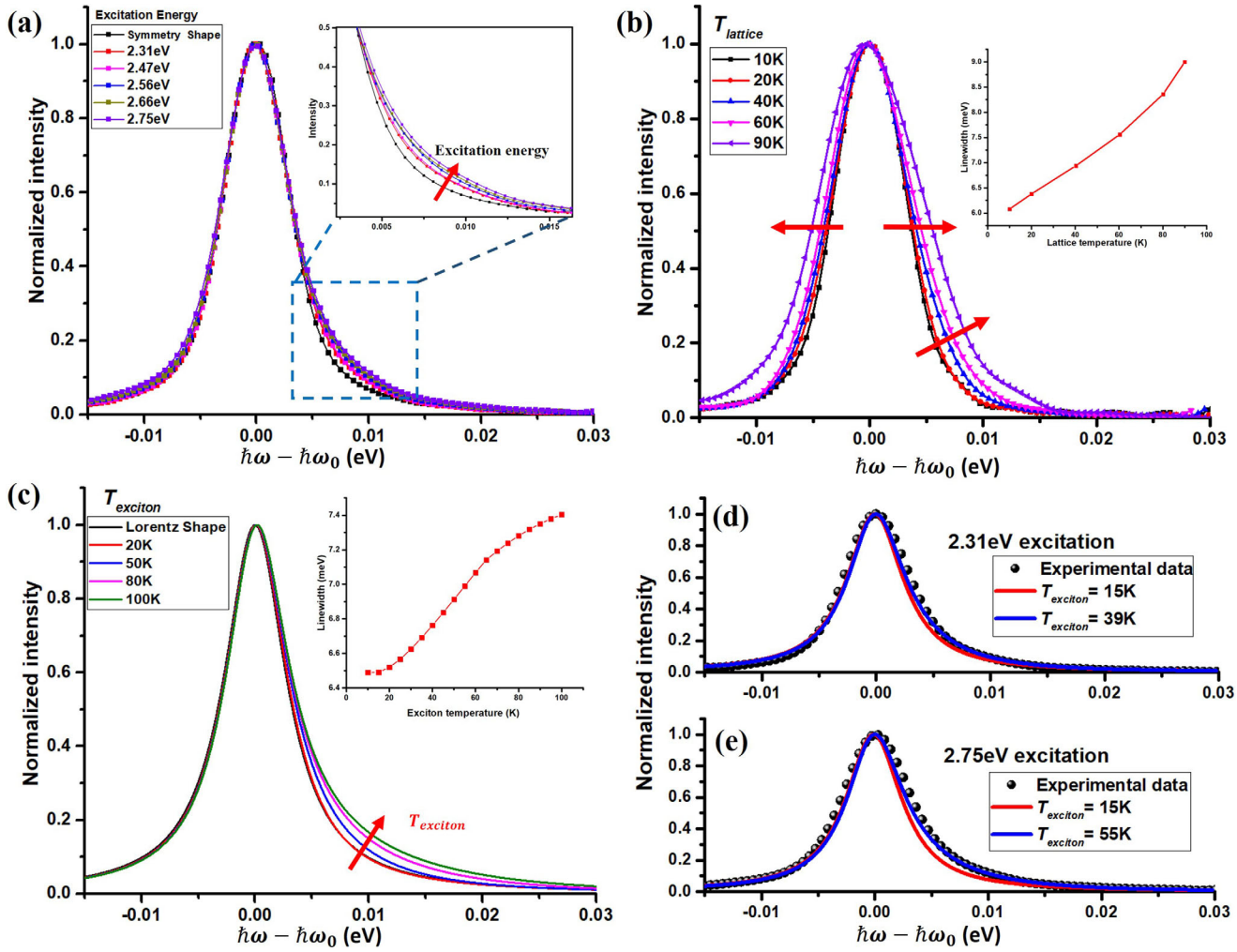

FIGURE 3 (a) Representative PL spectra under different excitation energies at 15 K base temperature. The PL spectra are renormalized and shifted with respect to the spectral peak for comparison. The upper halves of the PL lineshape (normalized PL > 0.5) are nearly the same, and the lower parts of PL lineshape expand at the higher excitation energy. The expansion weighs heavily at the higher energy tails as magnified in the inset. (b) Representative PL spectra at various cryostat temperature. The linewidth broadening owing to the lattice temperature displays different patterns against that of exciton temperature. The inset shows the linewidth from Lorentz fitting as a function of the lattice temperature (c) Simulated PL spectra with the mechanism of acoustic phonon-assisted exciton emission, where the lattice temperature is kept constant ($T_{lattice} = 15K$) and the exciton temperature is the sole variable. The high-energy side tail expands obviously accompanying with the linewidth broadening. The inset shows the linewidth broadening as a function of the exciton temperature. Simulation result of PL spectra with excitation energy of 2.31 eV (d) and 2.75 eV (e), the exciton temperature is estimated to be 39 and 55 K (~24 and 40 K higher than the lattice temperature) under the excitation energies of 2.31 eV and 2.75 eV, respectively

density monotonically decreases with the increasing excitation energy, the PL linewidth almost linearly increases. It seems contradictory to our excitation-intensity-dependent PL results (Figure 2b) if only the exciton density-induced linewidth variation is taken into account. We attribute this linewidth broadening to the APAPL, which we elaborate in the following section. In region II, the PL intensity remains flat, which implies the exciton density is nearly constant in region II and the exciton density-induced linewidth broadening could be excluded. Therefore, the APAPL plays a sole role in broadening the linewidth. Hence, the PL linewidth in region II increases faster than in region I (the two red lines in Figure 2d). Meanwhile, the Raman scattering is exploited to monitor the lattice temperature under the excitation (below 100 —W), showing that the local heating is negligible and the local lattice temperature remains a constant in the excitation range (details in the Supporting Information). The anomalous linewidth broadening in both regions I and II and the non-Lorentzian line shape of PL spectra are then attributed to the effective exciton temperature rise, which activates the APAPL process as demonstrated in Figure 3.

Figure 3a shows the representative PL spectra under different excitation energies. These PL spectra are renormalized and shifted with respect to the PL energy peak for better comparison. Note that the top halves of the PL spectra where the normalized intensity > 0.5 are nearly the same across the excitation energy range. Contrarily, the tail at the high energy side expands with the elevating excitation energy as illustrated in the inset. This linewidth broadening has a contrasting manner to the lattice temperature-induced line shape

26986248, 2023, 1, Downloaded from https://onlinelibrary.wiley.com/doi/10.1002/nts.20220035 by Cochrane Japan, Wiley Online Library on [13/01/2023]. See the Terms and Conditions (https://onlinelibrary.wiley.com/terms-and-conditions) on Wiley Online Library for rules of use; OA articles are governed by the applicable Creative Commons License

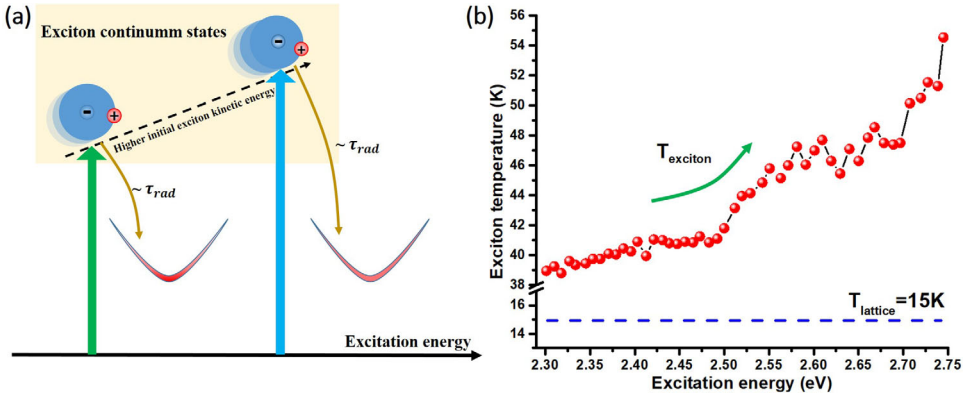

FIGURE 4 (a) Sketch of the relation between the effective exciton temperature and the excitation energy. The exciton excited by higher energy photon has a higher initial kinetic energy. After a time scale ($\sim\tau_{rad}$), the excitons reach different effective exciton temperatures. (b) The effective exciton temperature as a function of the excitation energy

broadening (Figure 3b), which displays a whole line shape broadening other than just an expansion in the tail. To simulate the phonon-assisted PL, we set the exciton temperature as the single variable and keep the lattice temperature as a constant (~15K). Figure 3c shows the simulated PL spectrum of *A*-1*s* exciton under the APAPL mechanism with all defined parameters from Glazov and Urbaszek's work[28] (detailed in the Supporting Information). The expansion at the higher energy edge leads to the effective linewidth broadening (inset of Figure 3c), remarkably reproducing the experimental features in Figure 2d. The simulation perfectly describes our experimental results, and it clearly indicates that the APAPL process makes significant contribution to the whole PL spectrum in high-quality samples. Comparing our experimental (Figure 3a) with simulation results (Figure 3c), we conclude that the higher excitation energy leads to the higher exciton temperature and finally raises non-Lorentz high-energy tail. As demonstrated in Figure 3d,e, the effective exciton temperature ($T_{exciton}$) is 24K higher than the lattice temperature ($T_{lattice}$) when the excitation is at 2.31 eV and 40 K higher at 2.75 eV, respectively.

Under higher energy excitation, excitons will have higher initial kinetic energy.[17] Within a typical exciton radiative lifetime τ_{rad}, the exciton reaches an effective exciton temperature ($T_{exciton}$), which is significantly different from the lattice temperature as sketched in Figure 4a. In Figure 4b, the effective exciton temperature is retrieved from the fitting of our PL spectra based on our model, which incorporates two components: one is the Lorentz function that describes the PL from the exciton inside the light cone; the other is the high-energy tail as elaborated in the Supporting Information, Note 6, which describes the APAPL ($T_{exciton}$ as a fitting parameter) from excitons outside the light cone. The latter contributes more weight as the $T_{exciton}$ increases. Our PLE experiments indicate that the effective exciton temperature can be tuned continuously by the excitation energy as shown in Figure 4b.

In summary, our PL and PLE spectroscopic experiments reveal that the effect of hot excitons and the effective exciton temperature can be remarkably extracted from the PL spectrum of monolayer TMDs. We elaborate the roles of effective exciton temperature and lattice temperature in PL spectra and the linewidth broadening mechanism. The thermal equilibrium between the excitons and the lattice is not necessarily achieved in linear optical properties of 2D TMDs. The effective exciton temperature could be tuned by excitation energy.

METHODS

Crystal growth

Bulk $MoSe_2$ crystals are grown by the chemical vapor transport method. Mo powder (99.9%), slightly excessive Se ingot (99.999%), and a bit of iodine as transport agents are loaded in silica tubes, which are evacuated and sealed. Then, the silicon tubes are put in the reaction zone of 950°C and the growth zone of 900°C. After 15 days, bulk $MoSe_2$ with large sizes are obtained in the cold zone. The monolayer $MoSe_2$ is mechanically exfoliated onto Si substrate with 285 nm SiO_2 film.

Sample preparation

Monolayer $MoSe_2$ and thin hexagonal boron nitride (hBN) were first exfoliated from bulk $MoSe_2$ crystal onto the different Si/SiO_2 (300 nm) substrates. Afterward, dry-transfer technique was used to stack them together. Figure S1 shows the optical image of our hBN-encapsulated $MoSe_2$ under bright and dark fields.

PLE measurement

In our PLE measurement, the light source (SuperK EXTREME EXB-3, NKT photonics) is a picosecond laser (80 MHz, 5 ps) pumped supercontinuum photonic crystal fiber going through a motorized continuous band-pass filter. The PL is collected through a long working distance

26986248, 2023, 1, Downloaded from https://onlinelibrary.wiley.com/doi/10.1002/nls.20220035 by Cochrane Japan, Wiley Online Library on [13/01/2023]. See the Terms and Conditions (https://onlinelibrary.wiley.com/terms-and-conditions) on Wiley Online Library for rules of use; OA articles are governed by the applicable Creative Commons License

objective (Olympus, 50x) with a spectrometer (Shamrock 193i) and an electron-multiplying charge-couple-device (EMCCD, Andor).

AUTHOR CONTRIBUTIONS

Conceptualization, formal analysis, investigation, software, project administration, visualization, writing-original draft: Ke Xiao. *Resources*: Ruihuan Duan. *Resources*: Zheng Liu. *Resources*: Kenji Watanabe. *Resources*: Takashi Taniguchi. *Writing-review and editing*: Wang Yao. *Conceptualization, funding acquisition, project administration, supervision, writing-review and editing*: Xiaodong Cui.

ACKNOWLEDGMENTS

The work was supported by the Hong Kong University Grants Council/ Research grants council under schemes of (AoE/P-701/20), GRF (17300520) and AoE seed fund of the University of Hong Kong and National Key R&D Program of China (2020YFA0309600). K.W. and T.T. acknowledge support from the Elemental Strategy Initiative conducted by the MEXT, Japan (Grant Number JPMXP0112101001) and JSPS KAKENHI (Grant Numbers 19H05790, 20H00354, and 21H05233). R.D and Z.L. acknowledge support from the Singapore Ministry of Education Tier 3 Programme "Geometrical Quantum Materials" AcRF Tier 3 (MOE2018-T3-1-002), AcRF Tier 2 (MOE2019-T2-2-105). The authors thank Dr. Fengren Fan, Dr. Tengfei Yan, and Dr. Bairen Zhu for the fruitful discussion.

CONFLICT OF INTEREST

Wang Yao is a co-author of the manuscript and an editor of Natural Sciences and was not involved in the handling of the peer-review process of this submission.

DATA AVAILABILITY STATEMENT

The data that support the findings of this study are available from the corresponding author upon reasonable request.

ETHICS STATEMENT

The authors confirmed that they have followed the ethical policies of the journal.

ORCID

Ke Xiao https://orcid.org/0000-0001-5260-7996

PEER REVIEW

The peer review history for this article is available at https://publons.com/publon/10.1002/ntls.20220035

REFERENCES

1. Chernikov A, Berkelbach TC, Hill HM, et al. Exciton binding energy and nonhydrogenic Rydberg series in monolayer WS 2. *Phys Rev Lett*. 2014;113:076802.
2. Ye Z, Cao T, O'Brien K, et al. Probing excitonic dark states in single-layer tungsten disulphide. *Nature*. 2014;513: 214-218.
3. Ugeda MM, Bradley AJ, Shi S-F, et al. Giant bandgap renormalization and excitonic effects in a monolayer transition metal dichalcogenide semiconductor. *Nat Mater*. 2014;13:1091-1095.
4. Zhu B, Chen X, Cui X. Exciton binding energy of monolayer WS_2. *Sci Rep*. 2015;5:9218.
5. He K, Kumar N, Zhao L, et al. Tightly bound excitons in monolayer WSe_2. *Phys Rev Lett*. 2014;113:026803.
6. Wang G, Marie X, Gerber I, et al. Giant enhancement of the optical second-harmonic emission of WSe_2 monolayers by laser excitation at exciton resonances. *Phys Rev Lett*. 2015;114:097403.
7. Mak KF, He K, Shan J, Heinz TF. Control of valley polarization in monolayer MoS_2 by optical helicity. *Nat Nanotechnol*. 2012;7: 494-498.
8. Zeng H, Dai J, Yao W, Xiao D, Cui X. Valley polarization in MoS_2 monolayers by optical pumping. *Nat Nanotechnol*. 2012;7:490-493.
9. Wang Z, Rhodes DA, Watanabe K, et al. Evidence of high-temperature exciton condensation in two-dimensional atomic double layers. *Nature*. 2019;574:76-80.
10. Sidler M, Back P, Cotlet O, et al. Fermi polaron-polaritons in charge-tunable atomically thin semiconductors. *Nat Phys*. 2017;13:255-261.
11. Zhang Y, Chang T-R, Zhou B, et al. Direct observation of the transition from indirect to direct bandgap in atomically thin epitaxial $MoSe_2$. *Nat Nanotechnol*. 2014;9:111-115.
12. Kormányos A, Burkard G, Gmitra M, et al. k·p theory for two-dimensional transition metal dichalcogenide semiconductors. *2D Mater*. 2015;2:022001.
13. Wellstood F, Urbina C, Clarke J. Hot-electron effects in metals. *Phys Rev B*. 1994;49:5942.
14. Chen Y, Li Y, Zhao Y, Zhou H, Zhu H. Highly efficient hot electron harvesting from graphene before electron-hole thermalization. *Sci Adv*. 2019;5:eaax9958.
15. Cortés E, Xie W, Cambiasso J, et al. Plasmonic hot electron transport drives nano-localized chemistry. *Nat Commun*. 2017;8:1-10.
16. Yan T, Yu H, Xiao K, Yao W, Cui X. Probing the exciton k-space dynamics in monolayer tungsten diselenides. *2D Mater*. 2019;6:025035.
17. Trovatello C, Katsch F, Borys NJ, et al. The ultrafast onset of exciton formation in 2D semiconductors. *Nat Commun*. 2020;11:1-8.
18. Wallauer R, Perea-Causin R, Münster L, et al. Momentum-resolved observation of exciton formation dynamics in monolayer WS_2. *Nano Lett*. 2021;21:5867-5873.
19. Hägele D, Zimmermann R, Oestreich M, et al. Cooling dynamics of excitons in GaN. *Phys Rev B*. 1999;59:R7797.
20. Wang L, Wang Z, Wang H-Y, et al. Slow cooling and efficient extraction of C-exciton hot carriers in MoS_2 monolayer. *Nat Commun*. 2017; 8: 1-8.
21. Kumar M, Vezzoli S, Wang Z, et al. Hot exciton cooling and multiple exciton generation in PbSe quantum dots. *Phys Chem Chem Phys*. 2016;18:31107-31114.
22. Hohlfeld J, Wellershoff S-S, Güdde J, Conrad U, Jähnke V, Matthias E. Electron and lattice dynamics following optical excitation of metals. *Chem Phys*. 2000;251:237-258.
23. Damen T, Leo K, Shah J, Cunningham J. Spin relaxation and thermalization of excitons in GaAs quantum wells. *Appl Phys Lett*. 1991;58:1902-1904.
24. Ziaja B, Medvedev N, Tkachenko V, Maltezopoulos T, Wurth W. Time-resolved observation of band-gap shrinking and electron-lattice thermalization within X-ray excited gallium arsenide. *Sci Rep*. 2015;5:1-7.
25. Umlauff M, Hoffmann J, Kalt H, et al. Direct observation of free-exciton thermalization in quantum-well structures. *Phys Rev B*. 1998;57:1390.
26. Moody G, Kavir Dass C, Hao K, et al. Intrinsic homogeneous linewidth and broadening mechanisms of excitons in monolayer transition metal dichalcogenides. *Nat Commun*. 2015;6:1-6.
27. Gupta G, Majumdar K. Fundamental exciton linewidth broadening in monolayer transition metal dichalcogenides. *Phys Rev B*. 2019;99:085412.
28. Shree S, Semina M, Robert C, et al. Observation of exciton-phonon coupling in $MoSe_2$ monolayers. *Phys Rev B*. 2018;98:035302.

26986248, 2023, 1, Downloaded from https://onlinelibrary.wiley.com/doi/10.1002/ntls.20220035 by Cochrane Japan, Wiley Online Library on [13/01/2023]. See the Terms and Conditions (https://onlinelibrary.wiley.com/terms-and-conditions) on Wiley Online Library for rules of use; OA articles are governed by the applicable Creative Commons License

29. Chow CM, Yu H, Jones AM, et al. Phonon-assisted oscillatory exciton dynamics in monolayer $MoSe_2$. *npj 2D Mater Appl*. 2017;1:1-6.
30. Helmrich S, Sampson K, Huang Di, et al. Phonon-assisted intervalley scattering determines ultrafast exciton dynamics in $MoSe_2$ bilayers. *Phys Rev Lett*. 2021;127:157403.
31. Lorchat E, Parra López LE, Robert C, et al. Filtering the photoluminescence spectra of atomically thin semiconductors with graphene. *Nat Nanotechnol*. 2020;15:283-288.
32. Cunningham PD, Hanbicki AT, McCreary KM, Jonker BT. Photoinduced bandgap renormalization and exciton binding energy reduction in WS_2. *ACS Nano*. 2017;11:12601-12608.
33. Pogna EAA, Marsili M, De Fazio D, et al. Photo-induced bandgap renormalization governs the ultrafast response of single-layer MoS_2. *ACS Nano*. 2016;10:1182-1188.
34. Liu F, Ziffer ME, Hansen KR, Wang J, Zhu X. Direct determination of band-gap renormalization in the photoexcited monolayer MoS_2. *Phys Rev Lett*. 2019;122:246803.
35. Qiu Z, Trushin M, Fang H, et al. Giant gate-tunable bandgap renormalization and excitonic effects in a 2D semiconductor. *Sci Adv*. 2019;5:eaaw2347.
36. Schaibley JR, Karin T, Yu H, et al. Population pulsation resonances of excitons in monolayer $MoSe_2$ with sub-1 μeV linewidths. *Phys Rev Lett*. 2015;114:137402.

SUPPORTING INFORMATION

Additional supporting information can be found online in the Supporting Information section at the end of this article.

How to cite this article: Xiao K, Duan R, Liu Z, et al. Hot exciton effect in photoluminescence of monolayer transition metal dichalcogenide. *Nat Sci*. 2023;3:e20220035. https://doi.org/10.1002/ntls.20220035

26986248, 2023, 1, Downloaded from https://onlinelibrary.wiley.com/doi/10.1002/ntls.20220035 by Cochrane Japan, Wiley Online Library on [13/01/2023]. See the Terms and Conditions (https://onlinelibrary.wiley.com/terms-and-conditions) on Wiley Online Library for rules of use; OA articles are governed by the applicable Creative Commons License